Interactive comment on "Aerosol Effects on Electrification and Lightning Discharges in a Multicell Thunderstorm Simulated by the WRF-ELEC Model" by Mengyu Sun et al.

M. Sun et al.

sunmengyu16@mails.ucas.edu.cn

Reply to Referee 2

General Comments:

The submitted paper is directed to study the effects of CCN concentration on lightning activity. Although the hypothesis of a link between the lightning frequency and CCN concentration is not new there are still only limited numbers of papers investigating the physical processes responsible for these links. However, the results of these studies are not unambiguous. Therefore, any further analysis in this direction (as is in the submitted paper) is well come for the scientific community. To reveal the effect of the CCN on microphysics and cloud dynamics and their impact on thunderstorm electrification and lightning, the authors present the results from numerical simulations with two different CCN concentrations: a polluted case (P-case) and a continental case (C-case). The Weather Research and Forecasting (WRF) Model coupled with bulk lightning model and a two-moment bulk microphysics scheme used to simulate a multicell thunderstorm is adequate for the aim of their study. The title corresponds to the content of the paper. The abstract is informative. Many recent and appropriate papers are cited in the Introduction. The paper as a whole is well structure. Most of the figures are of good quality. The analysis of the results of model simulations is directed to reveal the physical processes responsible for the significantly higher frequency of lightning in the P-case, as well as the earlier start of the discharge in the C-case. However, some conclusions are based on assumptions, rather than on detailed analyses of the corresponding numerical simulation results. A more comprehensive discussion, related to the mechanism by which the differences (due to the impact of CCN) in microphysics, thermodynamics, and cloud dynamics affect the electrification of clouds, is required. Additional information, figures and analyses are needed to convince the reader of the validity of the drawn conclusions. Based on the above I recommend the submitted paper to be revised taking into account the specific comments and recommendation below.

Response:

We greatly appreciate the instructive and constructive comments. We have studied them carefully and have addressed them in the revised manuscript. Below are the point-by-point responses to the reviewer's comments.

Specific Comments:

3. Model overview

It is necessary to provide additional information related to the numerical model and design of simulation, and not just direct the reader to the relevant papers.

On Ln 141-143 it is written: "The initiation of cloud droplets (both for cloud base and in-cloud) uses an expression based on Twomey (1959)." Please explain a little bit more and give the empirical expression proposed by Twomey (1959). Since the CCN spectra is approximated by power dependence on supersaturation using two time- and location-dependent coefficients, what were their specific values that you used in numerical simulations of C- and P-case? Does supersaturation threshold specified above which CCN number do not increase in the model?

Response:

Thanks for this comment. This comment contains 3 questions. We'll deal with them one by one.

(A) Regarding the description related to the initiation of cloud droplets:

The initiation of cloud droplets is based on Twomey (1959) and adjusted by Mansell et al. (2010). The number concentration initiated at cloud base is: $C_{N,cb} =$

$\frac{1}{\Delta t}10^6(10^6C)^{2/(k+2)}[\frac{1.63w^{3/2}}{kB(3/2,k/2)}]^{k/(k+2)}$, where C is the assumed CCN concentration, w is the updraft speed, B is the beta function, and k is the exponent in the relation $N_{CCN} = CS_w^k$, S_w is the supersaturation with respect to liquid water. Within the cloud, the initiation rate C_N is: $C_N = CkS_w^{k-1}\mathbf{V} \cdot \nabla S_w$.

(B) Regarding the CCN spectra:

We have added related information in the revise manuscript, for example:

Lines 150-153: "**The CCN concentration is predicted as a bulk activation spectrum and initially mixed well vertically, following Mansell et al. (2010):** $\boldsymbol{N_{CCN} = CCN \times S_w^k}$**, where CCN is the assumed CCN concentration,** $\boldsymbol{S_w}$ **is the supersaturation with respect to water, and k = 0.6**". And the assumed CCN concentration for both cases have been clarified in the revised version (lines 225-233).

(C) Regarding the supersaturation S_w:

For the first appearance of S_w at grid point, the mass of initiated droplets is calculated either by an iterative saturation adjustment or by one-step adjustment in Klemp and Wilhelmson (1978). Within the cloud, the vertical gradient of supersaturation is replaced with full gradient $[w(\partial S/\partial z) \rightarrow \mathbf{V} \cdot \nabla S_w]$. In this study, we apply no supersaturation adjustment and the threshold of that do not increase with CCN number in the model.

Ln 145-147 it is written:

"Non-inductive charge separation resulting from rebounding collisions between graupel-hail and snow-cloud ice are all parameterized (Mansell et al., 2005)". Instead of just directing the reader to the relevant paper, it is necessary to give additional brief information about the calculation of magnitude and sign of separated charge at non-inductive interaction of the hydrometeors. It is useful to be noted that the sign of the separated charge based on the results in Saunders and Peck (1998) depends not only on the cloud water content but on in-cloud temperature and on rime accretion rate, which in turn additionally depends on the mean fall velocity of riming ice particles. And it is also not correct that in Mansell et al., 2005 rebounding collisions between graupel-hail and snow-cloud ice are taken into account. In Mansell et al, 2005 it is written Charge separation rates are calculated for rebounding collisions of graupel with cloud ice and aggregate" and "No charge separation is calculated for rebounding collisions between snow aggregates and ice crystals". You should mention the rebounding collisions between various ice-phase particles (ice, graupel, snow, hail), which resulting in the separation of charge in the frame of your numerical simulations.

Response:

We agree to the suggestion and we have optimized the description according to the suggestions.

(A) Regarding additional information about the calculation of non-inductive charge separation:

We have added in the revised manuscript. (Revised version, lines 156-161)

(B) Regarding the rebounding collisions in Mansell et al. (2005):

Sorry for the inaccuracy. This description has been revised as suggested. (Revised version, lines 166-170)

Give also additional information related to the discharge model parametrization – i.e. how the electric field is simulated, what is the prescribed breakdown threshold, the values of the cylinder cross section C in eq.1, how the net total charge density is altered after the discharge and others. In section 4.5, where you analyze the reasons leading to delay in charge onset in P-case you pay special attention to the area in which the total charge density is > +0.1 nC m^{-3} or < -0.1 nC m^{-3}. It can be assumed that this is related to some basic assumption at lightning parametrization in the numerical model. If so, it must be also explained in section 3. Model overview.

Response:

Thanks for this comment. We have added the description as suggested. For example:

Lines 184-186: "**A flash would be initiated when the electric field exceeds a breakdown threshold, which variants of vertical electric profile of Dwyer (2003) at a model grid point**".

Lines 198-199: "**C the cylinder cross sectional area (set in the following simulations to radius R = 12 km (Fierro et al., 2013))**".

Lines 188-190: "**If the space charge magnitude at a grid point exceeds a specific space charge threshold (0.1 nC m^{-3} herein), this grid point will be involved in discharge within the cylinder during this time step.**"

Please, explain also how the effective radius of various hydrometeors (presented in Fig.7) is calculated.

Response:

Thanks for this suggestion. The related method has been added as follows: "**The domain-average mean-mass $radius_h$ of hydrometeors in Table is calculated following Eq. (7):**

$$radius_h = [\frac{1}{c_h} \times \frac{Sum(\rho_{air}(i,j,k) \times q_h(i,j,k))}{Sum(\rho_{air}(i,j,k) \times n_h(i,j,k))}]^{1/3}, \quad (7)$$

where ρ_{air} is the air density, and c_h, q_h, n_h are the density, mass concentration, and number concentration of hydrometeor species h (Mansell et al., 2010), respectively." (revised version, lines 315-319) We noted that this is domain-averaged mean-mass radius instead of "effective" radius. So we modified it to "domain-averaged mean-mass radius".

The information on the initial and boundary conditions given on line 166-168, namely: "The nested model configuration for the simulations are shown in Table 1. The 1°×1°NCEP GFS (Global Forecast System) data is used to establish the initial and boundary conditions." is insufficient. You should specify the starting time and the hourly interval (1h, 3h, or more hours) updates of GFS data used for your numerical simulations. I do not understand why do you use 1 °×1 ° NCEP GFS data instead of 0.25 °×0.25 ° (or at least 0.5 °×0.5 °) GFS data. And please explain, how do you perform nesting technique from a domain with a resolution of roughly 100 ×100 km to a domain with a resolution of 6 ×6 km?

Response:

Thanks for the comment. This comment contains 3 suggestions. We'll deal with them one by one.

(A) Regarding the information on the initial and boundary conditions:

We checked the simulations and found that 0.5 °×0.5 ° NCEP GFS data was used for the initial and boundary conditions. We have corrected this mistake in the revised version.

(B) Regarding the starting time and the hourly interval updates of GFS data:

In our revised version, we have added the related information. (Revised version, lines 216-220)

(C) Regarding how to perform nesting technique:

The WRF Preprocessing System (WPS, shown in Figure R1) is used to configure real-data simulations. First, we use "geogrid" program to define dimensions and horizontal resolution of domains (here we set the 6 km and 2 km nests). "Geogrid" also provides values for static fields at each model grid point. And then, the "ungrib" program is deployed to read GRIB files (a WMO standard file format for storing regularly-distributed fileds) and extract meteorological fields (Vtables are used to extract fields). Finally, we use the "metgrid" program to interpolate meteorological data (extracted by ungrib) to simulation domains (defined by geogrid) horizontally. More details could be found at: https://www2.mmm.ucar.edu/wrf/users/

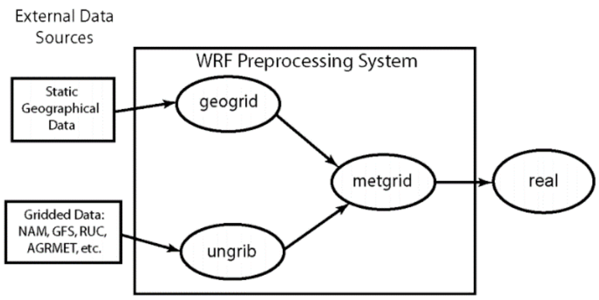

Figure R1 WPS program flowchart

4. Results

Before presenting the detailed analysis of the specific results, it would be useful to give the most general information about the simulated thunderstorms with two different CCN concentrations - at least the moment of the beginning of the formation of both simulated thunderstorms, their life time, the cloud base height, the maximum of cloud top height, the maximum updraft velocity, the amount of precipitation and others.

Response:

Thanks for this suggestion. We have added details of the simulated thunderstorms (Revised version, Table 2, 4). The precipitation information has been added as well. (Revised version, lines 254-272; Figure 6, 7)

4.1 Radar reflectivity and lightning flashes of multicell

The presented results in Fig. 2 and Fig 3 reveal that the numerical model used for the study of CCN impact on lightning activity adequately simulates some of the main manifestations of the real observed multicell thunderstorm. However, on the basis of this information alone, it is not possible to draw any other conclusions, including the statement in the last section, namely:

Ln 405-406 "The simulated distributions and spatio-temporal development of radar reflectivity are in overall agreement with observations." For this purpose, it is necessary to present at least observed radar reflectivity as a function of height in different stages of thunderstorm development with a 1.5-hour delay. And I assume that conclusion would be that the observed radar reflectivity is in agreement with simulated radar reflectivity only in the polluted case.

Response:

Thanks for this suggestion. We have presented the comparison of radar reflectivity for the observation and simulations at analyzed time (Figure 5 in revised version,), and added related description as follows: "**According to the morphology and intensity of the radar echo, the observed radar reflectivity is in better agreement with simulated radar reflectivity only in the polluted case.**" (Revised version, lines 247-249)

Since "the impacts of aerosol on lightning activity will only be evaluated in the southeastern Beijing area (116.0 °E-117.5°E)" (Ln 193-194) for clarity, denote in Fig. 2 the regions for which the results are analyzed. Please, explain how the presented in-cloud characteristics were averaged horizontally and in which region the lightning frequencies, shown in Fig.3 have been detected or simulated. It is useful also to specify the average rainfall only in the analyzed region?

Response:

Thanks for this comment. This comment contains 3 suggestions. We'll deal with them one by one.

(A) Regarding the analyzed region:

We have denoted in Figure 4d (revised version) the regions where the results are analyzed. And the spatial distributions of BLNET stations have been added in Figure 1 (revised version).

(B) Regarding the comparison of rainfall in the analyzed region:

The comparison of rainfall has been added in the revised version. (Lines 254-272; Figure 6, 7)

(C) Regarding the details of horizontal average process:

We have added in the revised manuscript as follows: "**For each quantity, the mass mixing ratio and number concentration of hydrometeors are averaged horizontally over the analyzed region at a given altitude.**" (Revised version, lines 312-314)

Ln 199-202

"According to the evolution of radar reflectivity and lightning activity, the thunderstorm was divided into four periods: the beginning stage (before 11:00 UTC), the developing stage (11:00-12:30 UTC), the mature stage (12:30-13:30 UTC) and the dissipating stage (after 13:30 UTC) of the thunderstorm" It is necessary to explain what the criteria were for determining the time intervals of the four stages of real and simulated development of a thunderstorm. I do not agree that lightning activity is suitable to be used for this purpose. An idea about the stages of thunderstorm development can be obtained for example on the basis of the evolution of heights of radar reflectivity 5 dBz and 45 dBz, the maximum radar reflectivity with the moment and height of its achievement. That is why I recommend to add such information (or something else) especially for the simulated C- and P-case. Based on chosen criteria, please give information for the corresponding four periods in the simulated C- and P-case and denote on the time scales in Fig.3b, Fig.5 (a-j), Fig.6 (a-d) the intervals of the mature stage in both simulated cases. This will facilitate to follow the analysis of the presented results and the conclusions drawn.

Response:

Thanks for this suggestion. In this study, the life cycle of the thunderstorm is determined according to the radar echo and lightning activities (Van Den Broeke et al., 2008; Kumjian et al., 2010, Liu et al., 2021). For the developing stage, the storm is accompanied with strengthened intensity and enlarged scale, with the lightning frequency increasing gradually. With regard to the mature stage, the maximum radar reflectivity at least reach 45 dBZ and the strong convective cell is formed, and the 15 dBZ echo top evaluate and the lightning frequency increase dramatically. As for the dissipating stage, the intensity of the storm is weakened with the 15 dBZ decreased, and the lightning frequency decreased remarkably. We have added the criteria and the real and simulated developments of the thunderstorm has been added. (Revised version, lines 277-279, Table2)

The conclusions made on the basis of the analysis of the results presented in Fig. 4, namely

Ln 217-221“There is no lightning initiation for the P-case at the beginning of the thunderstorm (08:30-09:30 UTC, Fig. 4a), however, all categories of lightning are initiated in the C-case, indicating that the first discharging is delayed under polluted condition.” are not unambiguous. It is necessary to indicate whether the delay of lightning initiation in the simulated P-case is due to the delay in the development of the thunderstorm or if the delay is due to another cause. For that reason, it would be useful if you present at least the evolution of cloud top height in P- and C-case starting from the early moment of thunderstorm formation before lightning initialization.

Response:

We appreciate this suggestion. In light of the following comment on the gap in the maximum radar reflectivity, we have analyzed the radar reflectivity and precipitation (Figure 6, 7, revised version) at the beginning stage of the thunderstorm for the observation and both simulations. Since the observed radar reflectivity during 11:00-11:24 UTC is missing, so Figure R2 shows the radar echo before and after 11:15 UTC (09:45 UTC in simulations) for comparison. In the early stage of the thunderstorm, the radar echo for the P-case is relatively similar with these of the C-case. We realized that the area we chose in the initial stage was too small. The extra cell in figure 5j (initial version) probably because that the previous selected area did not include the cell in the C-case. Therefore, we have enlarged the region (shown in Figure 4d, revised version). The microphysics along with further electrification and lightning activities of this thunderstorm have been re-analyzed. With such improvements, we believe the analysis of the physical processes is much appropriate for explaining the difference in the electrification and discharging in both simulated cases. The dynamic-thermodynamic processes do affect the development of thunderstorm significantly (e.g. Williams et al., 2005; Guo et al., 2016; Wang et al., 2018; Zhao et al., 2020), the re-analyzed results still suggest that under polluted condition lightning activity is significantly enhanced. While the delay of the first discharging in the C-case is not obvious. So we will delete this Part "4.5 Delay of first flash in polluted case" in the revised version. The detailed analysis of microphysical processes will be given in the following reply.

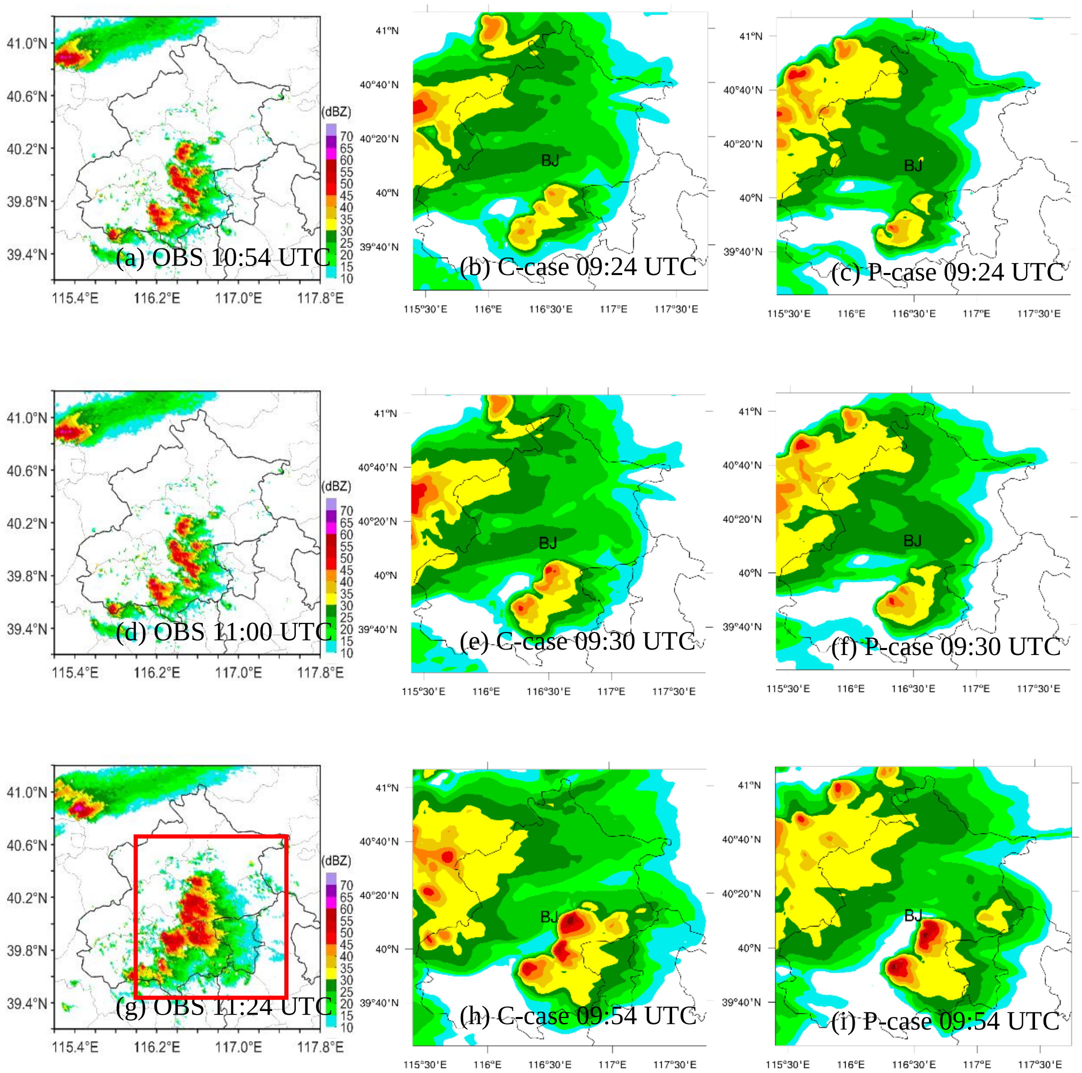

Figure R2 Radar reflectivity (unit: dBZ) between observation and simulation for the C- and P-cases, the simulation was earlier than observation about 1.5 h. (a), (d), (g) Observation at 10:54 UTC, 11:00 UTC and 11:24 UTC. (b), (e), (h) Simulation for the C-case at 09:24 UTC, 09:30 UTC and 09:54 UTC. (c), (f), (i) Simulation for the P-case at 09:24 UTC, 09:30 UTC and 09:54 UTC, respectively. The red rectangle in Fig. R2g denotes the region where the simulated results are analyzed in this study.

4.2 Microphysical properties of multicell

In Fig. 5 the vertical profiles of averaged horizontally mass mixing ratios and number concentration for different categories of hydrometeors as a function of time are shown for C- and P-case. No sound conclusions can be drawn for the impact of CCN concentration on cloud dynamics and microphysics on the basis of the horizontally averaged values alone. Information related to the corresponding maximum values, the height and time of their achievements has to be presented. For detailed analysis, it is also necessary to show additionally plots with the maximum values of updrafts and downdrafts as a function of time and height. I assume that the isolines of updrafts and downdrafts presented in Fig. 5i and 5j are horizontally averaged values, because they are too low for thunderstorms with an overshooting top, producing lightning. Please discuss also the reason for a gap in maximum radar reflectivity between 9:20 UTC and 10:00 UTC and between 10:30 UTC and 11:15 UTC in Fig. 5i. It will be also helpful if somehow the interval of the mature stage on the time scales in any of the plots in Fig. 5 is indicated. Why are there no plots of the mass mixing ratios and number concentration of snow and hail, especially considering that in section 4.3 the charge carried by these ice- particles is presented and discussed? And what about the simulated precipitation in C- and P-case? Please, add appropriate information and plots for example, peak rainfall rate (mm/h) as a function of time, total rainfall volume and others. Without such information, the analysis of the physical processes responsible for the difference in lightning frequency in both simulated thunderstorm cases is limited and the conclusions are not reliable.

Response:

Thanks for the comment. This comment contains 4 questions. We'll deal with them one by one.

(A) Regarding the information related to the maximum values, the height and time of updrafts and downdrafts

We have added the related figures and analysis. (Revised version, Lines 336-343; Figure 10i-10j; Table 4)

(B) Regarding the gap in maximum radar reflectivity between 9:20 UTC and 10:00 UTC and between 10:30 UTC and 11:15 UTC in Fig. 5i (initial version)

As mentioned before, we have re-analyzed the microphysical processes of the thunderstorm in the region denoted in Figure 4d. (Revised version, Part "**4.2 Microphysical properties of mulicell**", lines 309-385)

(C) Regarding to the mass mixing ratios and number concentration of snow and hail

The information of snow and hail have been displayed in Figure R3, R4 and summarized in Table R1. Yes, snow and hail are involved in the electrification. By collecting droplets and ice-phase particles, the aggregation of snow is partially similar to the accretion of graupel (Zrnic et al., 1993; Ziegler et al., 1985). The snow content is also less in the P-case (Figure R3a, R3b), while there is no significant difference of domain-averaged mean-mass radius of snow between the P- (421.1 μm) and C-case (375.9 μm, Table R1). The single graupel category, which has variable density in the microphysical scheme, represents a spectrum of particles ranging from high-density frozen drops (or small hail) to low-density graupel (Mansell et al., 2010), therefore, could better represent mixed-phase processes. After 12:00 UTC, the mean-mass radius of snow in both cases tend to increase (Figure R4a), which probably comes from the ice-phase particle conversion. Figure R3c-R3d display the temporal variations of the vertical profiles for hail in both cases. It can be seen that the difference of mixing ratio of hail between the two cases is not as obvious as that of graupel and ice crystals, during 10:00-13:00 UTC. The mean-mass radius of hail is slightly larger in the P-case (Table R1, Figure R4b). Small hail could be represented by frozen drops in the graupel category, whereas the hail category tends to represent larger hail (Bruning et al., 2007), this probably explains the little difference of hail between the two cases. Since there is little difference of number concentration and mean-mass radius compared to the graupel and ice crystal, we would add these to the supplement if necessary.

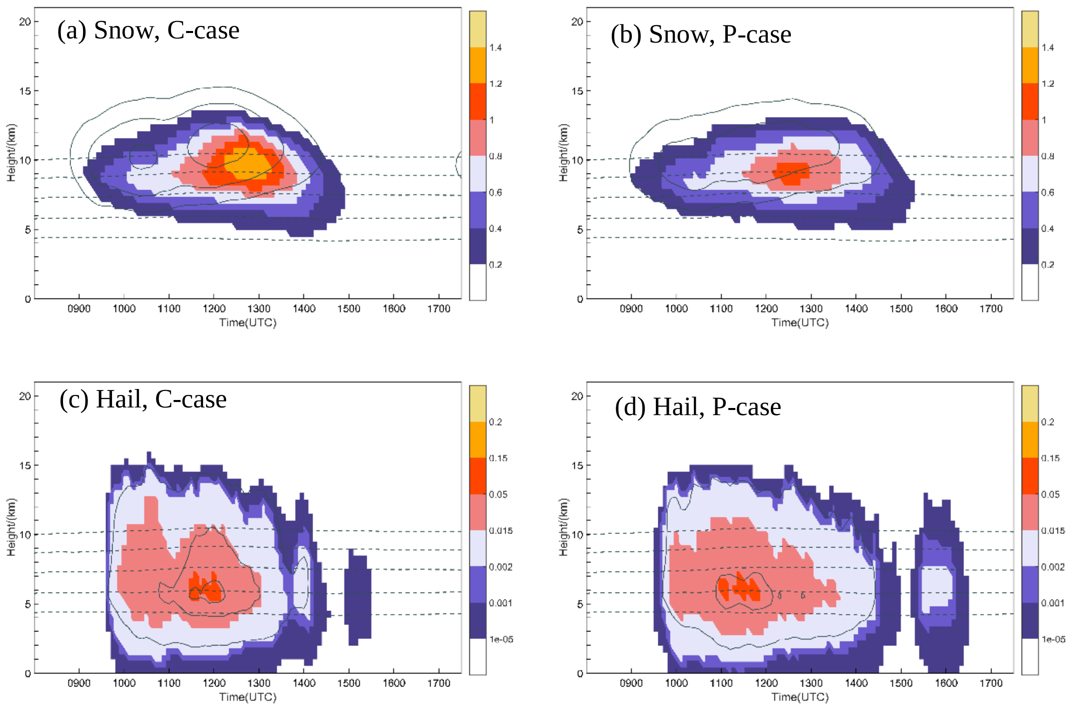

Figure R3 (a)-(d) Temporal variation of the vertical profiles of domain-averaged mass mixing ratio (g kg^{-1}, shaded) and number concentration (kg^{-1}, solid lines) of (a) snow in the C-case, (b) snow in P-case, (c) hail in the C-case, and (d) hail in the P-case. Contour levels in (a)-(b) for snow are 1.5×10^4, 3.0×10^4, 5.0×10^4 kg^{-1}, and for hail are 0.1, 1.0, 2.0 kg^{-1}. The 0 °C, -10 °C, -20 °C, -30 °C and -40 °C isotherms are shown by the dashed gray lines in (a)-(d).

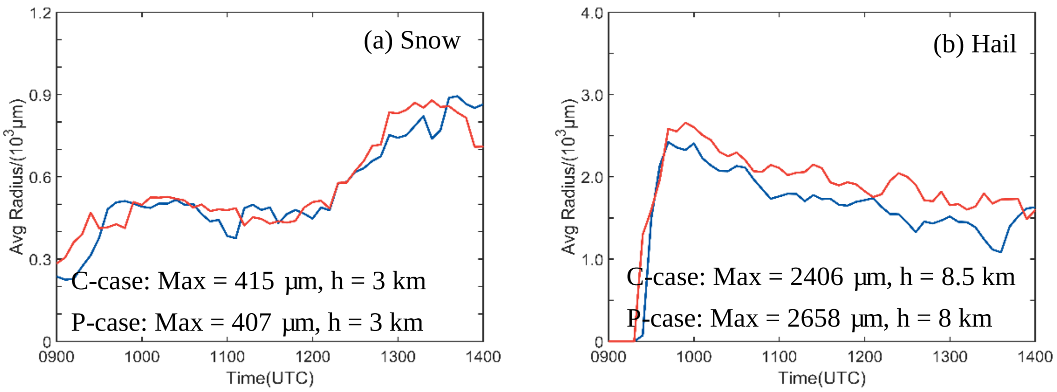

Figure R4 Temporal variation of domain-averaged mean-mass radius for the different hydrometeors. (a) snow, (b) hail. The red lines represent the P-case and the blue lines represent the C-case.

Table R1. Domain-averaged Properties of Hydrometeors.

	Number Concentration (10^3 kg^{-1})		Mean-mass Radius (μm)	
	C-case	**P-case**	**C-case**	**P-case**
Snow	4630	3880	375.9	421.2
Hail	0.00005	0.00004	1019.1	1248.6

(D) Regarding to the comparison of precipitation in the simulated C- and P-cases.

According to this suggestion, we have provided the comparison of precipitation for the observation and both simulations. (Revised version, lines 254-272; Figure 6, 7).

I do not understand for what reason the authors have decided first to consider the profile of total charge density and the charge carried by different ice-particles during the mature stage, then in the initial stage and without any attention to the impact of microphysics and dynamics of simulated clouds on their electrification during the maximum of lightning frequency. I do not think that it is appropriate to have separate sections - 4.4 Convective strength and 4.5 Delay of first flash in polluted case. All this can be presented in one section 4.3. The relationship between electrification, microphysics and dynamics. Again, the analysis presented in this section is cursory, often based on assumptions rather than on a profound investigation of the relation between microphysics, dynamics and thunderstorm charging. In order to get an idea about the formation of the charge structure during the different stages of thunderstorm development, it is appropriate to present horizontally averaged total charge density as a function of height and time, indicating for each of the stages of cloud development the maximum (minimum) positive (negative) total charge density together with the height and the moment of their achievement. Consideration of these results together with the results shown in Fig. 5 can give a general idea of the relationship between the mass of the ice-particles, updraft and downdraft velocity and time-height distribution of charge density in the polluted and in the continental case. In this analysis, it may be useful to pay attention to the time and amount of precipitation. And then to analyze the impact of microphysics and dynamics on thunderstorm electrification in 3 specific moments sequentially: at the initial moment of thunderstorm development (Fig. 11 and Fig.12), during the period of maximum lightning frequencies (it is necessary to show additionally appropriate figures) and finally during the mature stage (Fig. 7 and Fig.8) in the two simulated C- and P-cases. In my opinion, such a sequence of considerations would allow more detailed analysis to be made to clarify the processes responsible for the significantly higher lightning frequency in the P-case and the earlier onset of the discharge in the C-case. However, more comprehensive analyses have to be done, rather than only listing the results in the presented figures. For this purpose, it would be useful to look (at some specific moments of thunderstorms development) the profiles of the maximum updraft velocity and the mass of some hydrometeors related to thunderstorm charging.

Response:

We appreciated these valuable suggestions. This comment contains 2 suggestions. We will deal with them one by one.

(A) Regarding the analysis of charge density as a function of height and time.

We have added the temporal variation of the vertical profiles of peak positive (negative) charge density in the revised version (Figure 13). The WRF-ELEC outputs the total charge density after each discharge, so we chose to use peak charge density instead. In addition, we have added the related description. (Revised version, lines 388-398)

(B) Three specific moments: the initial moment, the mature stage, and the period of maximum lightning frequencies.

As mentioned before, we have re-analyzed the microphysics along with further electrification and lightning activities of this thunderstorm, in the region denoted in Figure 4d. The re-analyzed results still suggest that under polluted condition lightning activity is significantly enhanced, while the delay of the first discharging in the C-case is not obvious. And we would delete the Part “4.5 Delay of first flash in polluted case” in the revised version.

As shown in Figure 13 (revised version), the domain-averaged peak positive (negative) charge structures at the mature stage are similar with the period of maximum lightning frequency for both cases. And we have analyzed the vertical cross sections of simulated variables during the period of maximum lightning frequency (shown in Figure R5, R6, and R7), and found that the relationship between hydrometeors and electrification may not differ very much from the mature stage. For the total net space charge density, the maximum of positive charge density in the P-case (more than +1 nC m^{-3}, Figure R5a) is much higher than that in the C-case (less than +0.5 nC m^{-3}, Figure R6a), during the period of maximum lightning frequency. The collisions between ice particles and snow particles could partially explain the strong positive charge center located at 10-14 km in the P-case (Figure R5b). Less ice-phase particles appear in upper level in the continental case, corresponding to a relatively weaker charge center. In the polluted case, graupel and hail were charged negatively (Figure R7b, Saunders and Peck, 1998) with lower LWC, forming a negative charge center at 9km (< -20 ℃, shown in Fig. R5a). The appearance of more ice-phase particles in upper level, increasing ice crystals number and mean-mass radius of graupel, together led to greater charge densities and as a consequence to stronger electric field intensities. So we have only kept the related analysis at the mature stage in the revised version. (Lines 387-459, Figure 14, 15, and 16)

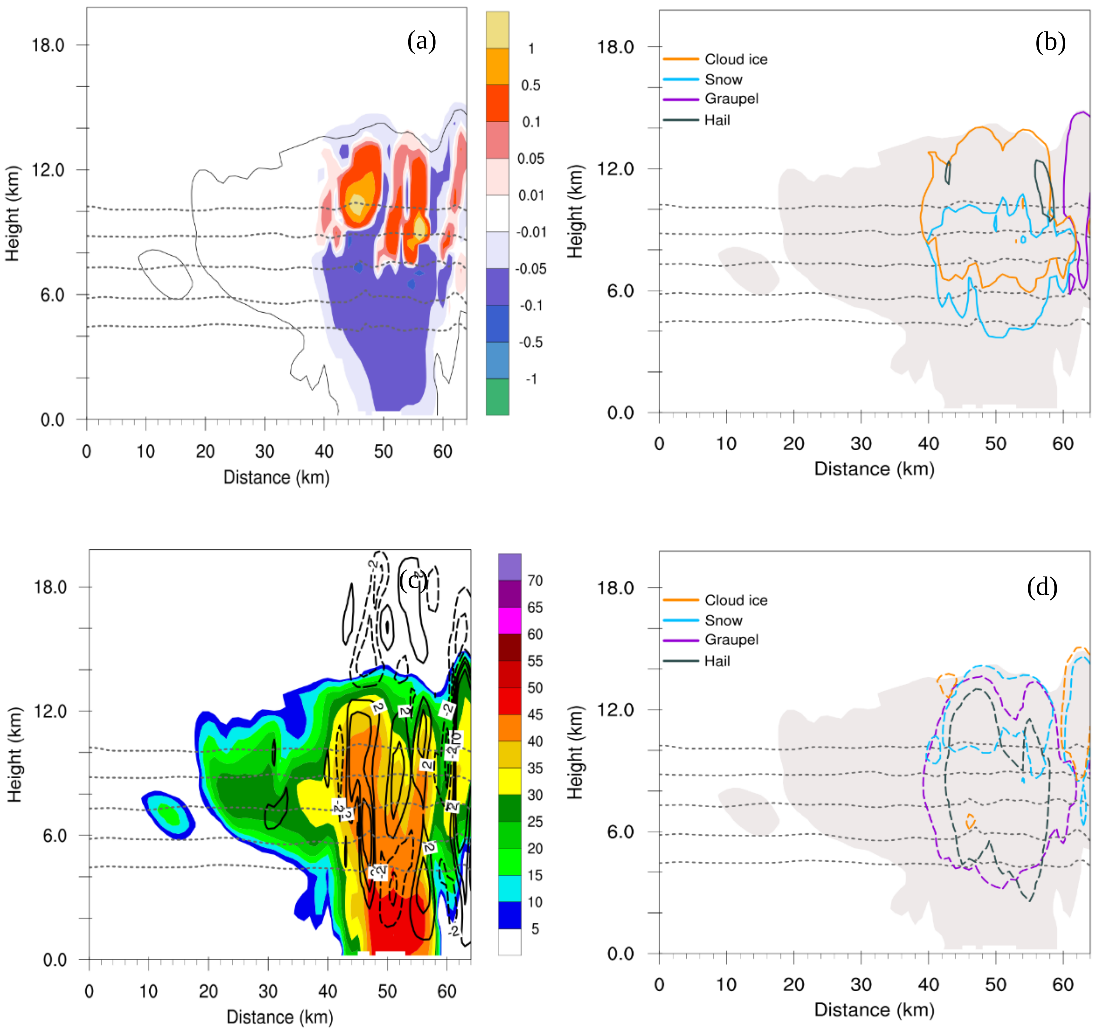

Figure R5 Vertical cross sections (south to north) at the location shown in Fig. 4f (revised version) of simulated variables during the period of maximum lightning frequency (10:36 UTC) in the P-case. (a) Total net space charge (nC m^{-3}, shaded). The 0 ℃, -10 ℃, -20 ℃, -30 ℃ and -40 ℃ isotherms are shown by dashed gray lines in (a)-(d). (b) +0.1 nC m^{-3} space charge density contours for cloud ice (orange), snow (blue), graupel (purple), and hail (black). The cloud outline (reflectivity echoes ≥ 5 dBZ) is denoted by the gray shaded contour. (c) Radar reflectivity (unit: dBZ), black lines for vertical velocities (solid line: 2, 5, 10 m s^{-1}; dashed line: -2 m s^{-1}). (d) As in (b), but for -0.1 nC m^{-3} charge density.

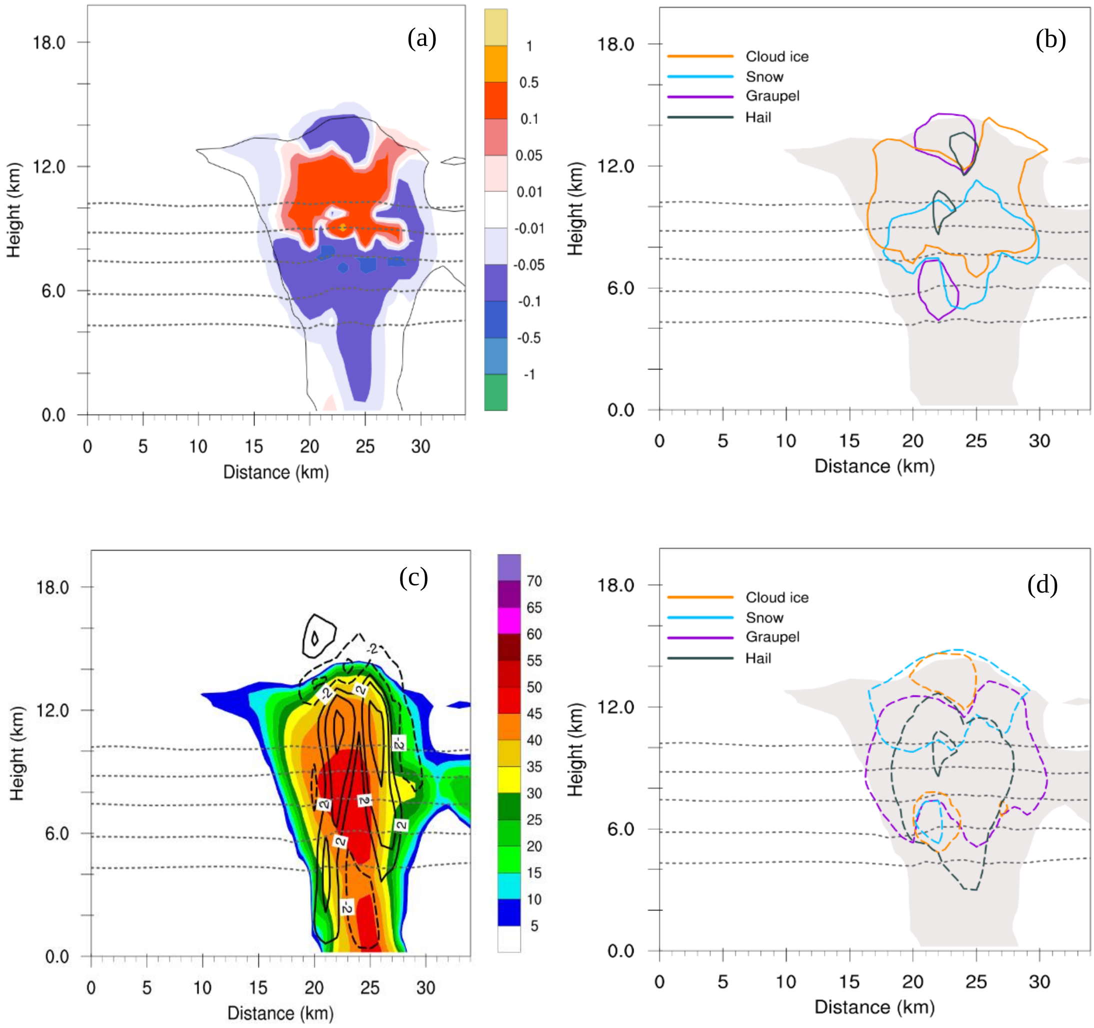

Figure R6 As in Fig. R5, but the vertical cross sections at the location shown in Fig. 4c (revised version) of simulated variables during the period of maximum lightning frequency (10:06 UTC) in the C-case.

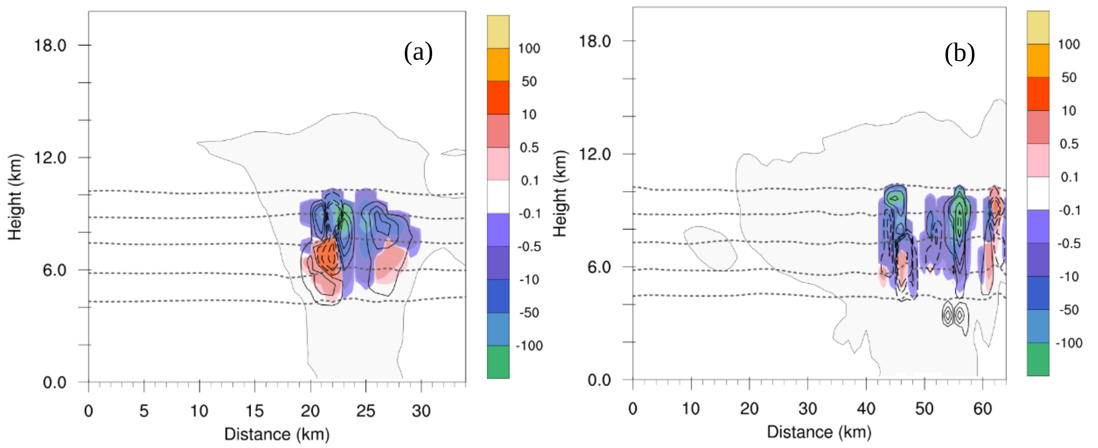

Figure R7 Vertical cross sections (south to north) at the locations shown in Fig. 4c and 4f (revised version) of non-inductive (pC m^{-3} s^{-1}, shaded) and inductive (solid lines: 0.1, 0.5, 1 pC m^{-3} s^{-1}; dashed lines: -0.1, -0.5, -1, -5, -10 pC m^{-3} s^{-1}) charging rates during the period of maximum lightning frequency (a) C-case (10:06 UTC, Fig. 4c), and (b) P-case (10:36 UTC, Fig. 4f). The 0 °C, -10 °C, -20 °C, -30 °C and -40 °C isotherms are shown by dashed gray lines.

Technical corrections:

1. Denote in Fig. 2 the regions for which the results are analyzed

2. The isotherms shown in the figures are very pale and difficult to see. It is also useful to show -30 ℃ and -40 ℃ isotherms.

3. The labels indicating the vertical velocities in Fig. 5 i and Fig.5j are blurred – they should be brighter.

4. It is better to use one and the same color for the results of C- and P-case simulation. So, it is desirable to use in Fig.4 (similar as in Fig.3b and in Fig.6) blue color for the C-case and red for the P-case.

5. The caption of Fig. 7 and others similar has to be revised because the figure does not show any microphysical characteristics.

Response:

Thanks a lot for these suggestions. All suggestions are helpful for us to improve our manuscript. We have modified in the revised version accordingly.

References:

Bruning E C, Rust W D, Schuur T J, et al. Electrical and polarimetric radar observations of a multicell storm in TELEX[J]. Monthly weather review, 2007, 135(7): 2525-2544.

Klemp J B, Wilhelmson R B. Simulations of right-and left-moving storms produced through storm splitting[J]. Journal of Atmospheric Sciences, 1978, 35(6): 1097-1110.

Kumjian M R, Ryzhkov A V, Melnikov V M, et al. Rapid-scan super-resolution observations of a cyclic supercell with a dual-polarization WSR-88D[J]. Monthly weather review, 2010, 138(10): 3762-3786.

Liu D, Sun M, Su D, et al. A five-year climatological lightning characteristics of linear mesoscale convective systems over North China[J]. Atmospheric Research, 2021, 256: 105580.

Saunders C P R, Peck S L. Laboratory studies of the influence of the rime accretion rate on charge transfer during crystal/graupel collisions[J]. Journal of Geophysical Research: Atmospheres, 1998, 103(D12): 13949-13956.

Van Den Broeke M S, Straka J M, Rasmussen E N. Polarimetric radar observations at low levels during tornado life cycles in a small sample of classic southern plains supercells[J]. Journal of applied meteorology and climatology, 2008, 47(4): 1232-1247.

Zrnic D S, Balakrishnan N, Ziegler C L, et al. Polarimetric signatures in the stratiform region of a mesoscale convective system[J]. Journal of Applied Meteorology and Climatology, 1993, 32(4): 678-693.